

## Chapter 4

# Heusler Alloys: Experimental and Theoretical Background

### 4.1 Introduction

The discovery of Heusler alloys dates back to 1903 when Heusler reported that the addition of *sp* elements (Al, In, Sn, Sb or Bi) turn Cu-Mn alloy into a ferromagnetic material even though the alloy contains none of the ferromagnetic elements [37]. The basic understanding of crystal structure and composition of these alloys remained unknown for a long time. In 1929 X-ray measurements of Potter [38] on Cu-Mn-Al alloy revealed that all constituents of this system was ordered on an fcc super lattice. Bradley and Rodgers [39] investigated Cu-Mn-Al system in detail using X-ray and anomalous scattering. The authors established a relationship between composition, chemical order and magnetic properties. After complete understanding of crystal structure numerous investigations were made. It is found that the Heusler structure is formed essentially from the ordered combination of two binary B2 compounds XY and XZ. Both compounds may have the CsCl type crystal structure, for instance CoMn and CoAl yield Co<sub>2</sub>MnAl. Thus the ability of compounds to form B2 structure indicates the possibility of forming new Heusler compounds. It was also discovered that it is possible to leave one of the four sublattices unoccupied (C1<sub>b</sub> structure). The latter compounds are often called half- or semi-Heusler alloys, while the L2<sub>1</sub> compounds are referred to as full-Heusler alloys. Extensive experimental studies showed that the majority of Heusler compounds order ferromagnetically in stoichiometric composition. Crystal structure, composition and heat treatment were found to be important parameters for determining magnetic properties.

With the discovery of half-metallic ferromagnetism in NiMnSb and the observation of shape memory effect in Ni<sub>2</sub>MnGa compound, Heusler alloys received tremendous experimental and theoretical interest. In this chapter we will briefly present the previous experimental and theoretical studies on structural and magnetic properties of Heusler alloys. Also, an overview of the experimental and theoretical studies on exchange coupling will be given.

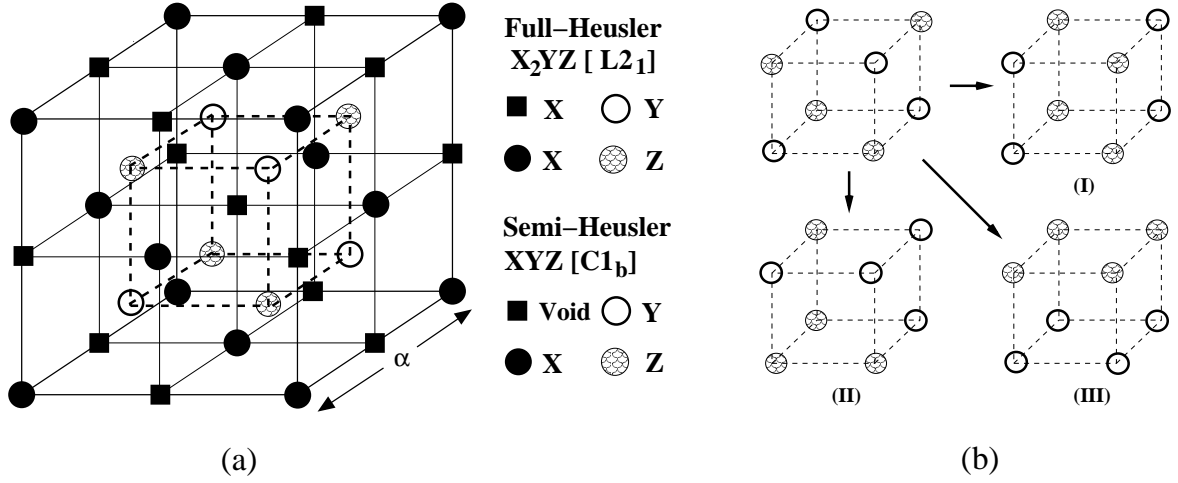


Figure 4.1: (a)  $C1_b$  and  $L2_1$  structures adapted by the half- and full-Heusler alloys. The lattice is consisted of 4 interpenetrating f.c.c. lattices. In the case of the half-Heusler alloys ( $XYZ$ ) one of the four sublattices is vacant. Note also that if all atoms were identical, the lattice would be simply the bcc. (b) Three possible configuration of the occupation of Y and Z sublattices in B2-type disordered structure.

## 4.2 Structural properties

Heusler alloys are defined as the ternary intermetallic compounds. At the stoichiometric composition, full Heusler alloys ( $X_2YZ$ ) and semi Heusler alloys ( $XYZ$ ) crystallize in  $L2_1$  and  $C1_b$  structures (see figure4.1), respectively. The elements normally associated with the X, Y and Z are indicated in table1. The unit cell consists of four interpenetrating fcc sublattices with the positions (000) and  $(\frac{1}{2}, \frac{1}{2}, \frac{1}{2})$  for X,  $(\frac{1}{4}, \frac{1}{4}, \frac{1}{4})$  for Y and  $(\frac{3}{4}, \frac{3}{4}, \frac{3}{4})$  for Z atom. The site  $(\frac{1}{2}, \frac{1}{2}, \frac{1}{2})$  is vacant in semi Heusler compounds. The two structures are closely related with vacant cite.  $C1_b$  structure can be obtained from  $L2_1$  one by replacing the half of the X sites in an ordered manner. Consequently, the structure no longer centro-symmetric. In majority of the Heusler alloys Mn element enters as the Y element. The compounds where Mn assumes the X positions are very rare. Up to now, only two systems of this type were studied experimentally:  $Mn_2VAl$  [40] and  $Mn_2VGa$  [41].

At the stoichiometric composition, disorder can exist in the form of partial interchange of atoms in different sublattices. Johnston and Hall [42] proposed a single disordering parameter  $\alpha$  to describe the effects of certain types of preferential disorder on the structure amplitudes of alloys of the type  $X_2YZ$ . For alloys ordered in  $L2_1$  structure  $\alpha$  is defined as the fraction of either Y or Z atoms being not on their correct sites. Partial occupation of Y and Z atoms on each others sublattices leads to  $L2_1$ -B2 type disorder. B2-type structure can be obtained by allowing half of the Y and Z atoms interchange their positions. The ratio of the  $L2_1$ /B2 depends on the heat treatments. Due to smaller interatomic distances in B2-type structure, an antiferromagnetic ordering becomes energetically favorable.

### 4.2.1 Martensitic phase transitions

At low temperatures several Heusler alloys, e.g.  $\text{Ni}_2\text{MnGa}$ ,  $\text{Co}_2\text{NbSn}$  etc., undergo a martensitic transition from a highly symmetric cubic austenitic to a low symmetry martensitic phase. Unlike atomic order-disorder transitions a martensitic transition is caused by non-diffusional cooperative movement of the atoms in the crystal [43]. It has been suggested that these transitions were driven by a band Jahn Teller mechanism [44] and there has not been any experimental evidence to confirm this conjecture for a long time. Recently the suggested model was confirmed by polarized neutron scattering experiments, where the transfer of magnetic moment from Mn to Ni was found in the martensitic phase of  $\text{Ni}_2\text{MnGa}$  [45, 46].

In the case when the Heusler alloys are magnetic in the martensitic phase, they can exhibit the magnetic shape memory effect (MSM). This occurs especially when the Y constituent is Mn, but other transition elements are also possible. In these alloys, an external magnetic field can induce large strains when applied in the martensitic state. Extensive experimental and theoretical investigations of the martensitic phase transition in the ferromagnet  $\text{Ni}_2\text{MnGa}$  have been made. This compound transforms martensitically at 202 K to a tetragonal structure below. There is a modulation of the (110) atomic planes with a periodicity of five atomic layers [50]. The transition is accompanied by a strong soft mode behavior in the transverse acoustic phonon branch with  $\mathbf{q}$  along the [110] direction and polarization along [1-10] in the high-temperature phase. Below the transition the system becomes magnetically anisotropic. In the martensitic phase of  $\text{Ni}_2\text{MnGa}$  an applied field of about 1 T can induce strains as large as 10% [47, 48]. The field induced strain is due to the reorientation of the tetragonal martensite variants by twin boundary motion [49].

## 4.3 Magnetic properties

Heusler alloys possess very interesting magnetic properties. One can study in the same family of alloys a series of interesting diverse magnetic phenomena like itinerant and localized magnetism, antiferromagnetism, helimagnetism, Pauli paramagnetism or heavy-fermionic behavior [50, 51, 52, 53].

### 4.3.1 Ferromagnets

The majority of the Heusler alloys order ferromagnetically and saturate in weak applied magnetic fields. If the magnetic moment is carried by Mn atoms, as it often is in the alloys  $\text{X}_2\text{MnZ}$ , a value close to  $4\mu_B$  is usually observed. Although they are metals, these compounds have localized magnetic properties and are ideal model systems for studying the effects of both atomic disorder and changes in the electron concentration on magnetic properties.

In order to reveal the role of the  $3d$  (X) and  $sp$  (Z) atoms on magnetic properties of Heusler alloys extensive magnetic and other measurements have been performed on quaternary Heusler alloys [50]. It has been shown that  $sp$  electron concentration is primarily

Table 4.1: Composition, magnetic order and crystal structure of Heusler alloys. The experimental information is taken from the reference [50].

Y	X	Z	Magnetic order	Crystal structure
V	Mn	Al, Ga	FM*	L2 <sub>1</sub>
	Fe	Al, Ga	FM	L2 <sub>1</sub>
	Fe	Si	PM	L2 <sub>1</sub>
	Co	Al, Ga, Sn	FM	L2 <sub>1</sub>
Cr	Co	Al, Ga	FM	L2 <sub>1</sub>
	Fe	Al, Ga	FM	L2 <sub>1</sub>
Mn	Cu	Al, In, Sn	FM	L2 <sub>1</sub>
	Cu	Sb	AFM	C1 <sub>b</sub>
	Ni	Al	AFM	B2
	Ni	Sb	FM	C1 <sub>b</sub>
	Ni	Al, Ga, In, Sn, Sb	FM	L2 <sub>1</sub>
	Co	Al, Si, Ga, Ge, Sn	FM	L2 <sub>1</sub>
	Co	Sb	FM*	C1 <sub>b</sub>
	Fe	Al, Si	FM	L2 <sub>1</sub>
	Pd	Al	AFM	B2
	Pd	In	AFM	L2 <sub>1</sub> -B2
	Pd	Ge, Sn, Sb	FM	L2 <sub>1</sub>
	Pd	Sb	FM	C1 <sub>b</sub>
	Pd	Te	AFM	C1 <sub>b</sub>
	Rh	Al, Ga, In	FM	B2
	Rh	Ge, Sn, Pb	FM	L2 <sub>1</sub>
	Rh	Sb	FM	C1 <sub>b</sub>
	Ru	Ga	FM	C1 <sub>b</sub>
	Au	Zn, Cu	AFM	B2
	Au	Al, Ga, In	AFM	L2 <sub>1</sub>
	Au	Sb	FM	C1 <sub>b</sub>
	Pt	Al, Ga	AFM	L2 <sub>1</sub>
	Pt	Ga	FM	C1 <sub>b</sub>
	Ir	Al	AFM	L2 <sub>1</sub>
	Ir	Ga	AFM	C1 <sub>b</sub>
Fe	Fe	Al, Si	FM	D0 <sub>3</sub>
	Co	Al, Si, Ga	FM	L2 <sub>1</sub>
Co	Fe	Ga	FM	L2 <sub>1</sub>
Ni	Fe	Al, Ga	PM	L2 <sub>1</sub>

FM\*:Ferrimagnetic

important in establishing magnetic properties, influencing both the magnetic moment formation and the type of the magnetic order.

In table 4.1 we present magnetic Heusler alloys containing  $3d$  transition metals (V, Cr, Mn, Fe, Co, Ni) as the Y site and  $3d$ ,  $4d$  and  $5d$  elements as the X site.

### 4.3.2 Antiferromagnets and ferrimagnets

Although the majority of Heusler alloys are ferromagnetic some of them order antiferromagnetically, in particular those compounds containing  $3d$  element in which the magnetic moment is only carried by Mn atoms at Y site. Experimentally antiferromagnetic order is measured both in semi Heusler (in  $C1_b$  structure) and in full Heusler alloys (in  $L2_1$  and B2 structure). Antiferromagnetism is more favorable in full Heusler alloys which has B2-type crystal structure due to smaller interatomic Mn-Mn distances. Indeed, antiferromagnetic behavior in several B2-type disordered  $X_2MnZ$  ( $X=Ni, Pd$ ;  $Z=Al, In$ ) Heusler alloys has been reported [50].

The situation is different in semi Heusler alloys. Due to large Mn-Mn distances in  $C1_b$  structure the antiferromagnetic interaction between Mn atoms is assumed to be mediated intermediate atoms (X or Z).

Ferrimagnetic ordering (antiferromagnetic coupling of X and Y atoms) is very rare in Heusler alloys compared to ferromagnetic or antiferromagnetic one. Ferrimagnetism has been detected [50] only in  $CoMnSb$ ,  $Mn_2VAl$  and  $Mn_2VGa$  compounds.  $Mn_2VAl$  received much experimental attention. The neutron diffraction experiment gave the ferrimagnetic state of compound with Mn magnetic moment of  $1.5 \pm 0.3\mu_B$  and V moment  $-0.9\mu_B$  [40].

### 4.3.3 Localized versus itinerant magnetism

Metals exhibiting local moment behavior are usually alloys and they are classified as disordered and ordered systems. Disordered alloys like Fe impurities in Cu or Ag have been intensively studied during the last four decades and a variety of magnetic behavior has been observed. Heusler alloys fall into the category of ordered systems. In these systems atoms carrying the magnetic moments are separated by other (usually non-magnetic) atoms and they are believed to carry well-defined local moments. The manganese moment, which is usually close to  $4\mu_B$ , remains fixed in amplitude when going from the ordered to the paramagnetic state. The formation of local moments in Heusler alloys will be discussed below.

A qualitative evidence for the localized magnetic behavior can be obtained by comparing ground state magnetic moment  $p_0$  with that extracted from the slope of the Curie-Weiss reciprocal susceptibility curve, i.e.,  $p_{eff} = \sqrt{p(p + 2\mu_B)}$ . A ratio  $p/p_0 \sim 1$  is expected for localized systems whereas for itinerant magnetism a ratio greater than 1 is expected. This allows one to analyze different mechanism for magnetic order. Indeed, a ratio close to one is obtained in several Heusler alloys [50] which reveals the nature of magnetism in these systems at least roughly.

The most direct quantitative evidence for localized magnetic behavior is provided by neutron scattering data. Measurements on  $\text{Pd}_2\text{MnSn}$ ,  $\text{Ni}_2\text{MnSn}$ ,  $\text{Cu}_2\text{MnAl}$  and  $\text{Pd}_2\text{MnIn}_{1-x}\text{Sn}_x$  Heusler compounds have been performed in order to study collective excitations [54, 55]. In all systems well defined spin waves were observed in the entire Brillouin zone below the Curie temperature  $T_c$  and highest energy at the zone boundary was approximately  $1-2T_c$ . Stoner excitations are well separated in energy from the collective excitations (spin waves) due to large exchange splitting  $\Delta$  ( $\Delta \sim 1-2 \text{ eV}$ ) and thus they can be neglected in consideration of thermodynamic properties. Also, measurements in the paramagnetic phase have established the absence of spatial magnetic correlations (spin waves), and have shown the value of atomic moment to be in agreement with that obtained from static susceptibility measurements.

However, the situation is different for those systems in which the moment is associated with the X atoms or both the X and Y atoms ( $\text{Co}_2\text{MnZ}$  or  $\text{Mn}_2\text{VAI}$ ). For such compounds the magnetic atoms are close enough for significant overlap of the  $d$  wave function to occur and there is then a tendency towards itinerant behavior [50, 51]. Hence Stoner excitations may be important.

## 4.4 Band structure calculations

The band structure calculations of Heusler alloys has been initiated by Ishida *et al.*, in the early eighties. The authors used non-self-consistent spherical augmented plane wave method (SAPW) to study electronic structure of  $\text{Ni}_2\text{MnSn}$ ,  $\text{Pd}_2\text{MnSn}$  [56] and  $\text{Cu}_2\text{MnAl}$  [57]. In 1983 Kübler *et. al.*, gave a detailed study on the formation and coupling of the magnetic moments in several Heusler alloys using self-consistent augmented spherical wave method (ASW). At the same year de Groot *et al.*, [59] discovered the half-metallic ferromagnetism in semi Heusler compounds  $\text{NiMnSb}$  and  $\text{PtMnSb}$ . Since then much effort has been devoted to the study of electronic and magnetic properties of these systems on the basis of band structure calculations.

### 4.4.1 Formation of local moments

The mechanisms of magnetic moment localization in transition metals and their alloys is one of the most interesting problems in modern magnetism. The origin of ferromagnetic behavior in Heusler alloys is rather complicated. The picture that emerged from the systematic calculations of Kübler *et. al.* for the microscopic mechanism responsible for the formation of magnetic moments in these systems is that the magnetization is very much confined to the Mn atoms [58]. The localized character of the magnetic moment results from the fact that the large exchange splitting of the Mn  $d$  states implies that Mn atoms support  $d$  states of only one spin direction. In the ferromagnetic state the spin-up  $d$  electrons of the Mn atom hybridize with those of the X atoms in forming a common  $d$  band, but spin-down  $d$  electrons are almost completely excluded from the Mn sites. Thus we are left with the completely localized magnetic moments composed of completely itinerant electrons. In figure 4.2 we

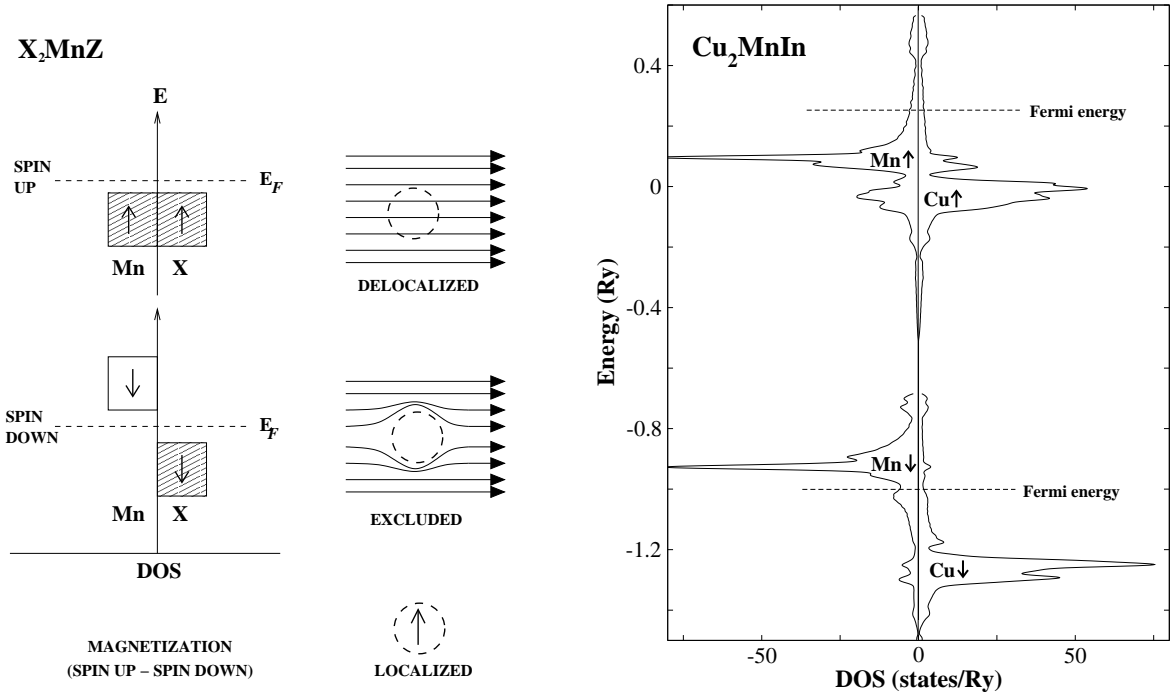


Figure 4.2: Left panel: Localized magnetic moments from delocalized electrons. Schematic diagram of up-spin and down-spin  $d$  electrons in Heusler alloys ( $X_2MnZ$ ) [58]. Right panel: The corresponding non-schematic site and spin projected  $d$  electron density of states for  $Cu_2MnIn$ .

present the physical picture that is just described. The same discussion is also valid for semi Heusler alloys (see next section).

Using the calculated total energies, it was possible to compare the relative stability of various magnetic phases (ferromagnetic one and two different antiferromagnetic ones) for a number of Heusler compounds [58]. Indeed, the magnetic moments of Mn atoms were found to be practically insensitive to the type of magnetic ordering. This behavior is obviously related to the localized nature of magnetism in these systems. Kübler *et al.*, also proposed that in full Heusler compounds,  $X_2MnZ$ , X atoms (e.g., Cu, Ni, Pd) serve primarily to determine the lattice constant, while Z atoms (Al, In, Sb) mediate the interaction between the Mn  $d$  states. However, experiments, particularly on quaternary systems have demonstrated that both X and Z atoms play similar role in establishing the magnetic properties [60, 61]. Furthermore, the magnetic properties are primarily determined by the conduction electron concentration.

#### 4.4.2 Half-metallic ferromagnetism

The concept of half-metallic ferromagnetism was introduced by de Groot *et al.*, on the basis of band structure calculations in NiMnSb and PtMnSb semi Heusler compounds [59]. In these materials one of the spin subbands (usually majority spin band) is metallic, whereas the Fermi level falls into a gap of the other subband (see Fig. 4.3). Ishida *et al.* have proposed that also the full-Heusler alloys of the type  $Co_2MnZ$ , ( $Z=Si, Ge$ ), are half-metals [62]. Since

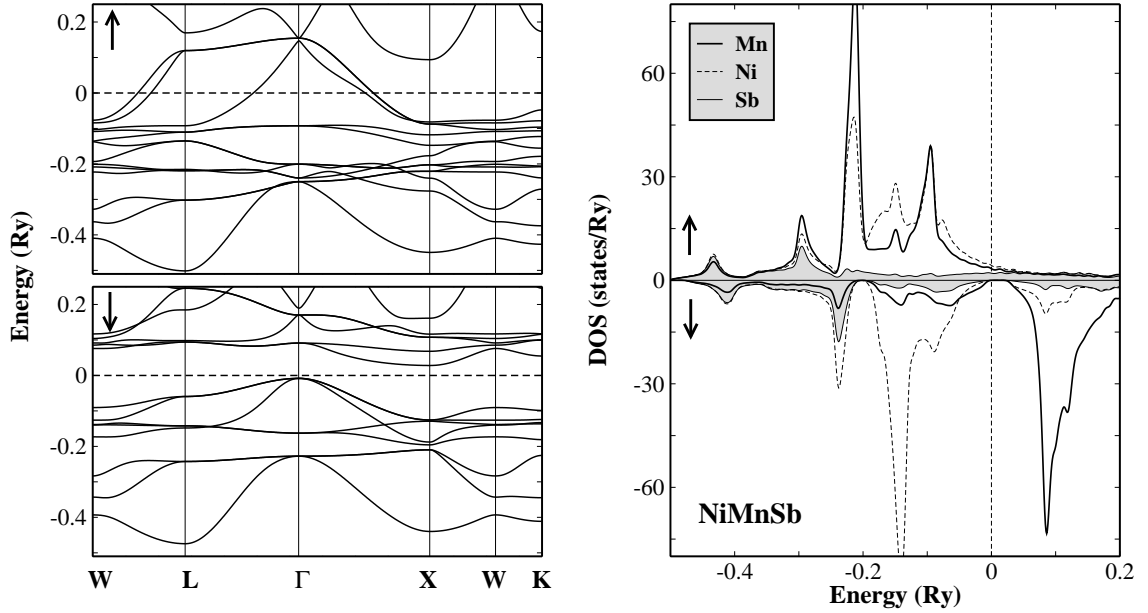


Figure 4.3: Left panel: Calculated band structure of half-metallic ferromagnet NiMnSb. The horizontal dashed line indicates the Fermi level. Right panel: Atom-resolved density of states (DOS) of NiMnSb. With shaded color we show the DOS of Sb.

then a number of further systems were predicted to be half-metallic. Among them are the binary magnetic oxides ( $\text{CrO}_2$  and  $\text{Fe}_3\text{O}_4$ ), colossal magnetoresistance materials ( $\text{Sr}_2\text{FeMoO}_6$  and  $\text{La}_{0.7}\text{Sr}_{0.3}\text{MnO}_3$ ) [63], diluted magnetic semiconductors ( $\text{Ga}_{1-x}\text{Mn}_x\text{As}$ ) and zinc-blende compounds  $\text{MnAs}$  and  $\text{CrAs}$  [64, 65, 66]. The origin of the appearance of half-metallic gap Heusler compounds will be discussed in detail in the following subsection.

#### • Origin of the half-metallic gap

The half-metallic ferromagnetism of semi Heusler alloys is intimately connected to their special so-called  $\text{C1}_b$  crystal structure and consequently the symmetry of the system. Due to a vacant site at the position  $(\frac{1}{2}\frac{1}{2}\frac{1}{2})$  in the  $\text{C1}_b$  crystal structure the symmetry of the systems is reduced to tetrahedral from the cubic in the case of  $\text{L2}_1$ -type full Heusler alloys. Thus the gap originates from the strong hybridization between the  $d$  states of the higher valent and the lower valent transition metal atoms [67]. This is shown schematically in figure 4.4. All Mn atoms are surrounded by six Z (Z is usually Sb) nearest neighbors (for the Mn atom at the (000) these neighbors are at  $(\frac{1}{2}00)$ ,  $(0\frac{1}{2}0)$ ,  $(00\frac{1}{2})$ ,  $(-\frac{1}{2}00)$ ,  $(0-\frac{1}{2}0)$  and  $(00-\frac{1}{2})$ ). As a result the interaction of Mn with the Z- $p$  states splits the Mn-3 $d$  states into a low-lying triplet of  $t_{2g}$  states ( $d_{xy}$ ,  $d_{xz}$  and a higher lying doublet of  $e_g$  states ( $d_{x^2-y^2}$ ,  $d_{3z^2-r^2}$ ). The splitting is partly due to the different electrostatic repulsion, which is strongest for the  $e_g$  states which directly point at the Z atoms. In the majority band the Mn 3 $d$  states are shifted to lower energies and form a common 3 $d$  band with X (X=Ni, Co) 3 $d$  states, while in the



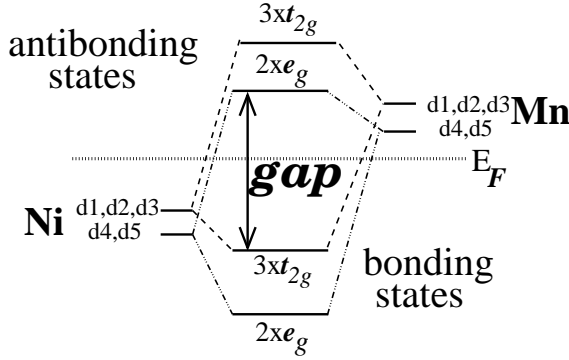


Figure 4.4: Schematic illustration of the origin of the gap in the minority band in semi-Heusler alloys [67].

minority band the Mn  $3d$  states are shifted to higher energies and are unoccupied, so that a band gap at  $E_F$  is formed, separating the occupied  $d$  bonding states from the unoccupied  $d$  antibonding states (see figure). Thus NiMnSb is a half-metal with a gap at  $E_F$  in minority band and a metallic DOS at the fermi level in majority band.

The calculated total magnetic moment is  $4 \mu_B$  per unit cell and mostly located in Mn atom. NiMnSb has 22 valance electrons per unit cell, 10 from Ni, 7 from Mn and 5 from Sb. Because of the gap at  $E_F$ , in the minority band exactly 9 bands are fully occupied (1 Sb-like  $s$  band, 3 Sb-like  $p$  bands and 5 Ni-like  $d$  bands) and remaining 13 electrons are accommodated in majority band resulting a magnetic moment of  $13-9=4 \mu_B$  per unit cell. Note that semi Heusler alloys like CoTiSb with 18 valence electrons shows semiconducting behavior.

It should be noted that the half-metallic character of semi Heusler compounds is highly sensitive to the crystal structure and symmetry e.g., the cubic point symmetry at Mn sites in ordinary  $X_2MnZ$  Heusler alloys gives rise to a symmetry of Mn- $3d-t_{2g}$  states that is different from the symmetry of the Sb- $p$  states. Hence, these states do not hybridize, so that no gap is opened in the minority spin band. The appearance of half-metallic ferromagnetism in full Heusler alloys is a subtle issue and explanation of it is very complicated. Recently Galanakis *et. al.* discussed this problem in detail [68].

#### • Slater-Pauling behavior

The total moment of the half-metallic semi- and full-Heusler alloys follows the simple rule:  $M_t = Z_t - 18$  and  $M_t = Z_t - 24$  where  $Z_t$  is the total number of valence electrons [67, 68]. The total number of electrons  $Z_t$  is given by the sum of the number of spin-up and spin-down electrons, while the total moment  $M_t$  is given by the difference  $Z_t = N_{\uparrow} + N_{\downarrow}$ ,  $M_t = N_{\uparrow} - N_{\downarrow}$ . Since 9 (12) minority bands of semi (full) Heusler alloys are fully occupied, a simple rule of 18 (24) is obtained for half-metallicity in  $C1_b$ -type ( $L2_1$ ) Heusler alloys.

This is analogues to the well-known Slater-Pauling behavior of the binary transition metal alloys [69]. The difference with respect to these alloys is, that in the half-Heusler alloys the minority population is fixed to 9 and 12, so that the screening is achieved by filling the majority band, while in the transition metal alloys the majority band is filled with 5  $d$ -states or completely empty and charge neutrality is achieved by filling the minority or majority

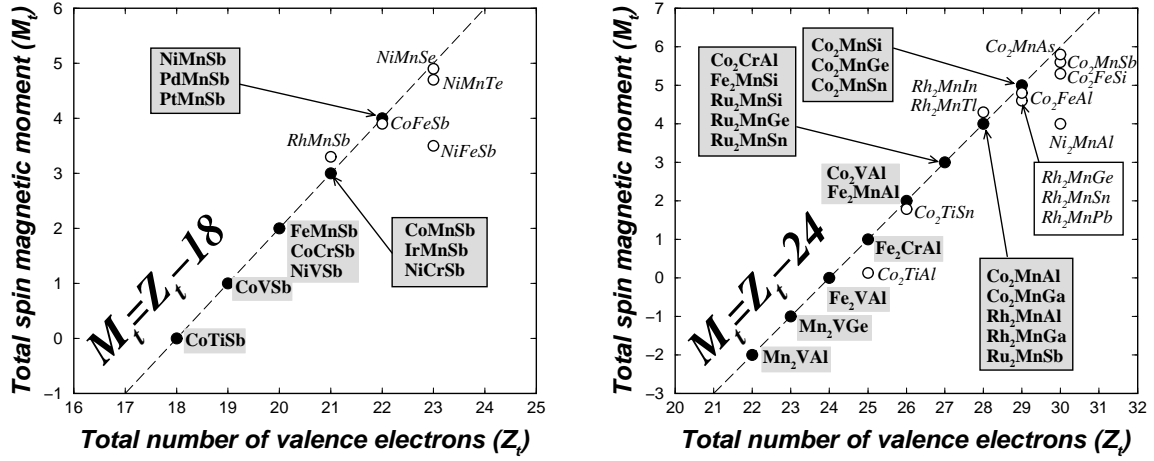


Figure 4.5: Left panel: Calculated total spin moments for semi Heusler alloys. The dashed line represents the Slater-Pauling behavior. Open circles indicates the compounds deviating from the SP curve [67]. Right panel: The same for the full Heusler alloys [68].

states. Therefore in the TM alloys the total moment is given by  $M_t = 10 - Z_t$  for the systems on the left side and  $M_t = Z_t$  for the systems on the right side of the Slater-Pauling curve.

For the half-metallic zinc-blende compounds like CrAs the rule is:  $M_t = Z_t - 8$ , since the minority As-like valence bands accommodate 4 electrons [70]. In all cases the moments are integer. In Fig. 4.5 we have gathered the calculated total spin magnetic moments for both Heusler alloys which we have plotted as a function of the total number of valence electrons. The dashed line represents the rule  $M_t = Z_t - 18$  ( $M_t = Z_t - 24$ ) obeyed by these compounds. The total moment  $M_t$  is an integer quantity, assuming the values 0, 1, 2, 3, 4 and 5 if  $Z_t = 18$ . In the case of full Heusler alloys ( $Z_t = 24$ )  $M_t$  can also take -2, -1 and 6. The value 0 corresponds to the semiconducting phase.

## 4.5 Exchange coupling: An overview

In view of the large separation of the Mn atoms ( $> 4 \text{ \AA}$ ) and available inelastic neutron scattering experiments in Heusler alloys, the electrons of the unfilled Mn 3d shell can presumably be treated as very well localized, so that the 3d electrons belonging to different Mn atoms do not overlap considerably. The ferromagnetism in these systems is thought to arise from an indirect interaction, by way of conduction electrons, between the Mn moments. The first important information on the exchange coupling in these systems is provided by the inelastic neutron scattering experiments of Noda and Ishikawa in the late seventies [54]. The authors measured the spin wave spectra of Ni<sub>2</sub>MnSn and Pd<sub>2</sub>MnSn for various directions in the Brillouin zone and analyzed the results within the Heisenberg model. The obtained results for the exchange parameters were in good agreement with the assumption of indirect exchange coupling in Heusler alloys. Indeed, the pattern of exchange interactions was oscillatory and

long range reaching beyond the eight nearest neighborhood distance.

This behavior of exchange interactions has been taken as an evidence for Friedel oscillations and the results have been interpreted using either an RKKY model

$$J_R = -\frac{9\pi n^2 I^2}{8E_F} \frac{\cos(2k_F R)}{(k_F R)^3} \quad (4.1)$$

or Hartree-Fock treatment of double resonance model

$$J_R = -\frac{25}{4S} E_F \sin^2 \phi^- \frac{\cos(2k_F R - 2\phi^-)}{(k_F R)^3} \quad (4.2)$$

where  $n$  is the number of conduction electrons,  $I$  is the s-d exchange constant,  $E_F$  and  $k_F$  are Fermi energy and wave vector, respectively, and  $\phi^-$  is the phase shift of the scattered wave function of the down spin electrons of the Mn atoms.  $\phi^-$  is given by

$$\phi^- = \frac{\pi}{5}(5 - n_B) \quad (4.3)$$

where  $n_B$  is the Mn magnetic moment divided by  $m_B$ .

Although both models gave good agreement with experiments for the exchange interactions at large distances, they were unable to account for either the sign and magnitude of the nearest and next nearest neighbor exchange parameters. The failure of these models for close distances was attributed to the involved asymptotic approximations. Price, however, showed that double resonance model unrestricted by any asymptotic approximation was able to capture qualitative features of the observed spin wave spectra in  $\text{Pd}_2\text{MnSn}$  [71]. Malmström and Geldart discussed the effect of the finite spin distribution on the RKKY interaction between the Mn moments [72]. The authors showed that, in spite of simplified treatment of electron band structure, finite spin distribution could bring the calculated values of the exchange interactions into agreement with that determined for the  $\text{Ni}_2\text{MnSn}$  and  $\text{Pd}_2\text{MnSn}$  compounds from the experimental studies. Reitz and Stearns, in addition to indirect *s-d* coupling, proposed two more coupling mechanisms to achieve agreement with experimental data: *d-d* exchange between itinerant and localized *d* electrons and super exchange via the Z atoms [73]. This model was capable of accounting for a wide range of properties in many different compounds because of the arbitrary adjustable parameters in latter mechanisms.

It is worth to note that all these model Hamiltonian approaches have certain advantageous and disadvantageous. The most prominent useful feature of them is that they provide a qualitative physical picture of magnetic interactions and reveal different intrinsic parameters for the mediation of exchange interactions between Mn atoms such as the number of conduction electrons, their polarization and finite spin distribution around Mn atoms. On the other hand, the main drawback of such approaches become obvious when one tries to predict the properties of new systems. This is mostly due to large number of arbitrary parameters and the use of simplified band structure model. Complete information on the magnetic interactions in solids can be, in principle, obtained from the solution of the Schrödinger equation as discussed in the preceding chapters.

The first quantitative study of the exchange interactions in Heusler alloys is given by Kübler *et al.*, within parameter free density functional theory [58]. The authors proposed a mechanism of super exchange type via the diamagnetic group III-V elements responsible for the Mn-Mn coupling. The calculation of the Mn-Mn exchange parameters is based on the comparison of the ferromagnetic and antiferromagnetic configurations of the Mn moments within the super cell relying on the Heisenberg model with localized moments. Although this approach works very well for systems with short range exchange interactions, i.e, interactions do not reach beyond the second nearest neighborhood (since in this case exchange parameters can be easily obtained from few magnetic configurations with the use of small super-cells), the situation is very different for systems with long range exchange coupling. In this case one needs large super cells and quite large number of magnetic configurations to extract all exchange parameters which obviously makes calculations very complicated and very expensive. This is also why Kübler *et al.*, reported only first two nearest neighbor exchange parameter in Heusler alloys, although they are known to be quite long range from experiments. It should be, however, noted that, in principle the obtained exchange parameters from simple calculations appear as the sum of all parameters if they are long range. Furthermore, within this method one can exactly get on-site exchange parameter  $J_0 = \sum_{\mathbf{R}} J_{0\mathbf{R}}$ , but this does not provide any information about the distribution of exchange parameters. Among the further findings of the Kübler *et al.*, is the absence of the considerable direct overlap of Mn 3d wave functions in Heusler alloys. The discussion is based on the comparison of the density of states for ferromagnetic and antiferromagnetic configurations.

Consequently, although the calculations of Kübler *et al.*, were an important step, however they were not able to explain the observed spin wave spectra of Heusler alloys. The most quantitative treatment of the exchange interactions in ferromagnets became possible after the implementation of the non-collinear magnetism in modern electronic structure codes. Developments in this field yields reliable and efficient calculation of exchange interactions up to the arbitrary distance from a magnetic atom in the crystal.

Coming back to the discussion of microscopic mechanisms for indirect exchange coupling in Heusler alloys we see on the the basis of model Hamiltonian approaches that two main points are central to understand them: conduction electrons and their spin polarization. Since the problem of interaction between local moments is rather closely connected with the problem of conduction electron polarization around a magnetic moment. To clarify this issue it is important to obtain information on the conduction electron spin polarization, and important information in this regard is provided by measurement and analysis of the hyperfine fields in non-magnetic sites (X,Z) in several Heusler alloys. The strength of the transferred hyperfine fields correlates with the amplitude of the *s* conduction electron polarization. Indeed measurements by Campbell and Khoi *et al.*, showed that maximum conduction electron polarization is found in the systems with high Curie temperatures such as Cu<sub>2</sub>MnAl and Cu<sub>2</sub>MnIn [74, 75].

However, hyperfine fields are only sensitive to the *s* electron polarization and do not

say anything about the polarization of  $p$  electrons which are dominated in Heusler alloys and expected to play the same role as  $s$  electrons. To probe the whole conduction electron polarization we have to resort to another method. Compton scattering profiles are proved to be quite useful tool in this respect. Indeed, using this method, recent measurements of Zukowski *et al.*, on  $\text{Cu}_2\text{MnAl}$  gave a large  $sp$  electron polarization which is antiferromagnetically coupled to Mn moment [76]. Also similar result is obtained for  $\text{Ni}_2\text{MnSn}$  by Deb *et al.*, [77].